Effect of Solvent Balance on the Surface Properties of Poly(vinyl chloride)

GARY C. WILDMAN* and S.-J. RAYMOND HSU, *Department of Polymer Science, University of Southern Mississippi, Hattiesburg, Mississippi 39406*

Synopsis

Films of poly(vinyl chloride) have been cast from solutions of varying thermodynamic quality and the film properties studied by inverse phase gas chromatography. The solvents included tetrahydrofuran, cyclohexanone, and mixtures of toluene with both tetrahydrofuran and cyclohexanone. The solvent composition was followed during evaporation and film formation for the mixed solvents, and it was shown that the slower evaporating solvent component has the greatest effect on the surface properties of the films. The porosity of the polymer film surfaces is interpreted in terms of the mobility of the polymer chains during film formation. At high concentrations, polymer chain–polymer chain interactions become stronger when thermodynamically less powerful solvents are used or are last to leave during film formation; therefore, the solvent balance has a critical influenece on the film surface properties. Annealing the poly(vinyl chloride) above the glass transition temperature reduces the surface porosity of the cast polymer.

INTRODUCTION

The surface structure and properties of polymeric materials are known to be of significant importance in determining their applications in the fields of coatings and adhesives. Recently intensive efforts attempting to characterize polymer-surface properties have been made both qualitatively and quantitatively by using different approaches, such as electron spectroscopy for chemical analysis (ESCA),[1] infrared spectroscopy,[2] laser Raman spectroscopy,[3] microscopy,[4] contact-angle measurements,[5] etc.

The introduction of inverse phase gas chromatography (IGC) in 1969 by Smidsrod and Guillet[6] added a new dimension to investigating polymer-surface properties. Recently, Schreiber and Croucher[7] reported on the surface properties of several solvent-cast polymers by the use of IGC. Their findings indicated that a good solvent produces a tightly packed film due to the relatively extended chains in the good solvent; on the other hand, thermodynamically less efficient solvents yield a more porous film because the polymer chains are more tightly coiled and intramolecular interactions are favored.

However, some authors[8–11] indicate that in good solvents polymer-chain dimensions decrease rapidly initially and then gradually with increasing polymer concentration, and become in accord with the unperturbed chain

*Present Address: Scholl, Inc., P. O. Box 377, Memphis, TN 38151.

Journal of Applied Polymer Science, Vol. 30, 4385–4408 (1985)
 CCC 0021-8995/85/114385-24$04.00

dimensions in the bulk state. In other words, in concentrated solutions the radius of gyration of polymer chains in a good solvent is similar to that in a poor solvent. Obviously this finding is in contrast to the interpretation which was employed by Schreiber and Croucher to draw conclusion on the solvent effects on polymer-film properties.

To help resolve this question, in this investigation a second point of view is attempted; namely, the packing ability of polymer chains during film formation is a function of their own mobility in concentrated solutions. Furthermore, the changes of solvent composition during film formation were ignored, and only the intrinsic viscosities in the initial stage of film formation were used to relate the polymer-chain dimensions in their report. Unfortunately, for solvent mixtures the solvent composition varies with time before and during film formation.[12] Any change of solvent composition prior to the solidification of the polymer film could significantly affect the film properties. In the previous work, no attempt was made to identify the point of solidification and determine the solvent composition at this moment. In this investigation, the change in solvent composition before film formation was carefully studied using gas chromatography. The results showed that this approach provides valuable information in supporting the interpretation of surface property differences arising from the use of different solvents in polymer-film preparation.

In this investigation, solvent balance was emphasized and two different series of solvents were employed to study their effects on solution properties of high concentrations as well as surface properties.

EXPERIMENTAL

Materials

Poly(vinyl chloride) (PVC) was purchased from Aldrich Chemical (18958-8, Lot #AB03) which had a viscosity average molecular weight of 74,000 in tetrahydrofuran ($K=1.5 \times 10^{-4}$dL/g, $a=0.77$). The glass transition temperature (T_g) was determined to be 83°C from differential scanning calorimeter (DSC, DuPont 910) measurements using a scan speed 10°C/min. Methanol, toluene, tetrahydrofuran (THF), cyclohexanone (CHO), dodecane, carbondisulfide, and chlorobenzene were of spectroquality grade. Chromosorb W (AW-DMCS treated, 80–100 mesh) was used as received.

Preparation of Solutions

Two different series of solvent mixtures were used for preparing PVC solutions. The first is referred to as the THF series, which represents five different volume-percent ratios of THF/toluene, i.e., 100/0, 90/10, 80/20, 70/30, and 60/40. The second is the CHO series, which has the same volume ratios of CHO/toluene as that of THF series. Solutions of 1 and 5% PVC were prepared by dissolving 1 and 5 g of PVC in 100 mL of each solvent mixture in the THF and CHO series. The solutions were then heated to 50°C for 24 h to ensure the complete dissolution.

Intrinsic Viscosity

The intrinsic viscosity measurements were made at 25 ± 0.01°C using a Cannon-Fenske size 50 viscometer.

Low Shear-Rate Viscosity

The low shear-rate viscosity measurements were made at three temperatures, 298, 306, and 318 K, by using Cannon-Ubbelohde four-bulb shear dilution capillary viscometers (sizes 50, 100, and 150). The viscosity η was related to the flow time t by the following equation[13]: $\eta = Ct$, where C is the viscometer constant. The shear rate at the wall of the capillary, γ (s^{-1}), was obtained from the equation[14]: $\gamma = K/t$, where K is the shear-rate constant of each bulb.

Determination of Solvent Evaporation

Internal Standard Calibration

Known weight ratios of THF, toluene, CHO, and the internal standard, chlorobenzene, were prepared and chromatographed. Gas chromatographic analyses were performed with a Hewlett-Packard Model 5710A equipped with a flame ionization detector. A stainless steel column with dimensions of 10 ft in length and 0.125 in. in diameter, packed with 80/100 W AW-DMS I98926, was used for this analysis. The area of each peak was measured by the triangulation method[15] as shown for the toluene peak in Figure 1.

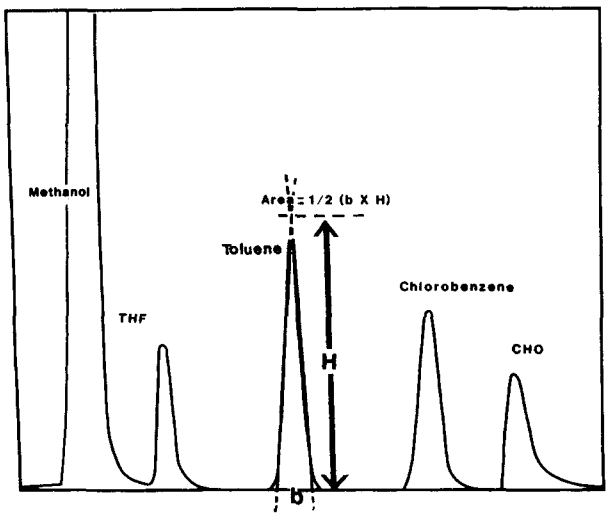

Fig. 1. A typical chromatogram for internal standard calibration. Conditions: injection port temp 250° C; detector temp 300° C; oven temp 120° C; flow rate 6 mL/min.

A typical chromatogram for internal standard calibrations is illustrated in Figure 1. In addition, the area ratios of solvents/standard are plotted against their own weight ratios to generate the calibration curves shown in Figure 2.

Determinations of Solvent Compositions During Solvent Evaporation

For each 1% THF series solution, 20 samples of 0.221±0.002 g of 1% PVC solution were weighed in 10-mL vials, and for CHO series the weights were changed to 0.231±0.002 g due to the higher density of CHO. Next, all of the vials were uncapped at the same time under good ventilation. Then, two vials for each solution were capped in every time interval sequentially. As soon as the vials were capped, 0.5 mL of THF was injected into each capped vial of CHO series or 0.5 mL of CHO into THF series to dissolve any possible solid PVC formed during the period the vial was uncapped. Then the PVC in each vial was precipitated by adding 2 mL of methanol, which contained 0.00537 g/mL chlorobenzene as an internal standard. Finally, the compositions of the residual solvents were quantitatively analyzed by using gas chromatography and the internal standard curves shown in Figure 2.

Surface Characterization by Inverse Phase Gas Chromatograph

The same chromatograph was used as described above. The PVC was coated on the inert support, Chromosorb W, from a 1% solution first by slowly evaporating the solvent with the filteration method described by Supina,[16] and then drying the packing to a constant weight under vacuum at room temperature. The PVC-coated supports were resieved and packed into a 1 m long, 2.1 mm i.d. stainless steel tubing which had previously been washed with methanol. The column then was conditioned in the gas chromatograph oven under a nitrogen flow at ca. 60°C for 10 h before use. Column temperature was controlled by submerging the column in a 30°C water bath. The specific retention volume V_g^0 was calculated by the following equation[17]:

$$V_g^\circ = \frac{ft_r}{W}\frac{273}{T_r}\frac{P_o - P_w}{P_o}\frac{3}{2}\frac{(P_i/P_o)^2 - 1}{(P_i/P_o)^3 - 1}$$

where f is the flow rate (mL/min) of the carrier gas, nitrogen, which was measured at an ambient temperature T_r (K) by using a soap bubble flow meter, P_w is the vapor pressure of water at T_r, P_i is the pressure at the column inlet which was measured with a mercury manometer, P_o is the pressure at the column outlet which was assumed to be approximately equal to the atmospheric pressure, W is the PVC loading weight (g) which was usually between 3 and 4%, determined by calcination,[18] and t_r is the net retention time which was taken at the point where the base line intersects with the tangent of the greatest slope for the front side profile of the probe (dodecane) peak.[17] A typical chromatogram is shown in Figure 3.

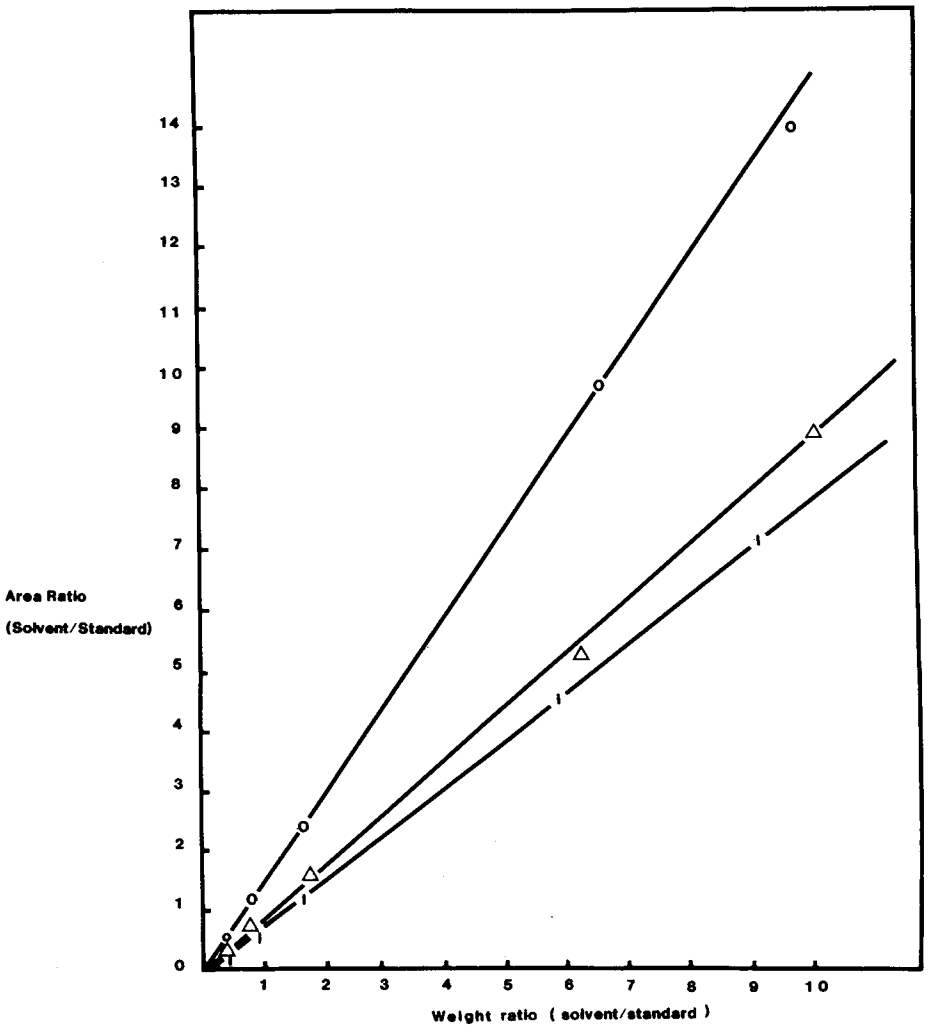

Fig. 2. Calibration curves for gas chromatograph analysis. Standard, chlorobenzene: (|) THF (tetrahydrofuran); (○) toluene; (△) cyclohexanone.

After measurements had been made at 30°C, the columns were baked at 90°C for 3 h with a nitrogen flow, and the measurements were repeated.

RESULTS AND DISCUSSIONS

Intrinsic Viscosity

As shown in Table 1, the intrinsic viscosity of PVC at 25°C in different mixed solvents decreases with the increasing volume percentage of toluene. In other words, the increased amount of toluene in solvent mixtures makes the solvent thermodynamically less efficient and leads to a smaller radius gyration of polymer chains.

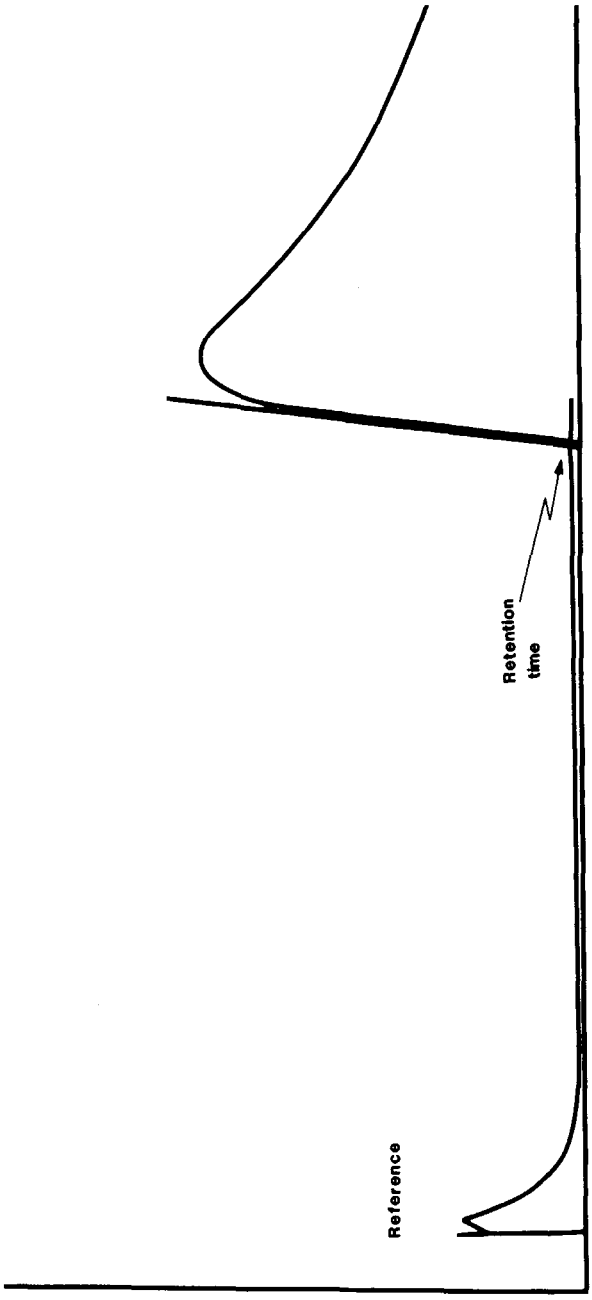

Fig. 3. A typical chromatogram in IGC analysis. Conditions for running IGC: column temp = 30°C in water bath; detector temp = 300°C; injection port temp = 250°C; carrier gas flow rate = 15 mL/min.

TABLE I
The Intrinsic Viscosity of PVC in THF- and CHO-Series Solvents

Solvent[a]	Intrinsic viscosity
THF	0.845
THF 90	0.830
THF 80	0.818
THF 70	0.786
THF 60	0.765
CHO	0.853
CHO 90	0.842
CHO 80	0.827
CHO 70	0.808
CHO 60	0.791

[a] Solvent code: THF = tetrahydrofuran; THF 90 = 90% THF/10% toluene; THF 80 = 80% THF/20% toluene, etc.; CHO = cyclohexanone; CHO 90 = 90% CHO/10% toluene, etc.

Low Shear-Rate Viscosity

In this investigation, it was found that the viscosities of PVC solutions are independent of shear rate at the range of shear rates measured. These data are shown in Figure 4. This fact means that flow times were always long enough that kinetic energy corrections were unimportant, and that non-Newtonian effects were absent.[19] The specific viscosities η_{sp}, were calculated by the following equation[20]: $\eta_{sp} = (\eta - V_s\eta_s)/\eta_s$, where V_s is the volume fraction of solvent and η_s is the viscosity of the solvent. The results of these measurements and calculations are listed in Table II and plotted in Figures 5 and 6. As can be seen from the change of specific viscosities v. the concentrations of PVC solutions for both the THF- and CHO-solvent series, the specific viscosities of PVC solutions at 25°C increase with the increasing volume percentages of toluene in mixed solvents when the PVC solutions which contain a larger percentage of toluene give a larger specific viscosity as long as the concentrations are higher than a certain level. In general, the viscosity is considered as an energy loss process which occurs when interacting molecules move relative to each other. Consequently, any process which causes neighboring molecules to move must contribute to the macroscopic viscosity of an assembly of molecules.[21] Also, it has been known that the motion of polymer chains will be dominated by the presence of direct polymer chain–polymer chain interactions or entanglements in nondilute solutions.[22] Based on this understanding, the increase in specific viscosity is associated with the stronger entanglements[20] or the stronger interactions[23] between the polymer chains which leads to a larger energy dissipation. Furthermore, according to the study of steady-state compliance by several investigators,[20,24,25] the density of entanglement coupling is independent of the solvent nature in higher concentrations; the higher specific viscosity in a poor solvent is believed to be due to the larger interchain interaction strength in poor solvents. Therefore, the motion of polymer chains in poor solvents is more restricted than that in good solvents. This characteristic of solution properties may be one of the important factors responsible for film properties.

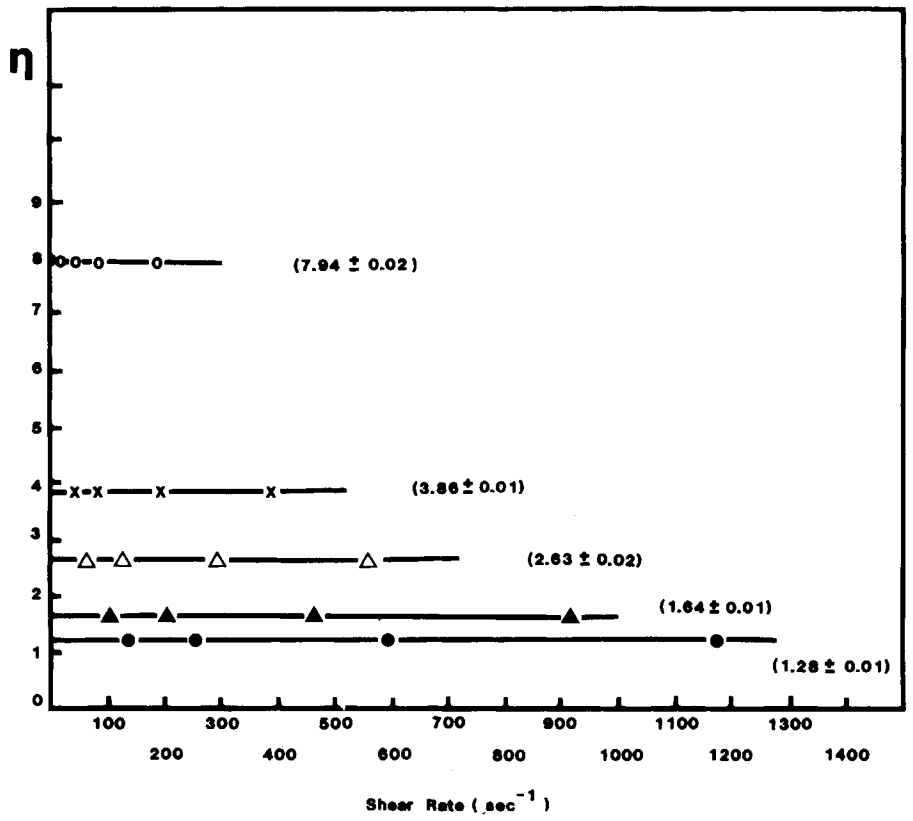

Fig. 4. The viscosity of PVC solutions as a function of shear rate. Viscosity (cS) at 25°C for PVC in pure THF: (○) 5% solution; (X) 3.33%; (△) 2.5%; (▲) 1.67%; (●) 1.25%.

Calculations of Activation Energy for Polymer Chain Motion

To support the viewpoint that polymer chains have larger interactions or entanglements in a thermodynamically less efficient solvent, measurements of low shear-rate viscosity were made at two other temperatures, 306 and 318 K in addition to the data collected at 25°C (298 K). The activation

TABLE II
Specific Viscosity in Various Solvents at Different Concentrations at 25°C

Concn (W/V%)	THF	THF 80	THF 60	CHO	CHO 80	CHO 60
5.00	14.07	15.52	19.36	13.11	13.56	15.75
2.50	4.01	4.16	4.43	3.85	3.97	4.13
1.67	2.12	2.24	2.30	2.08	2.16	2.38
1.25	1.43	1.52	1.51	1.43	1.49	1.56
1.00	1.04	1.01	1.01	1.01	1.02	1.03
0.50	0.466	0.460	0.445	0.463	0.463	0.458
0.25	0.225	0.219	0.218	0.236	0.232	0.217

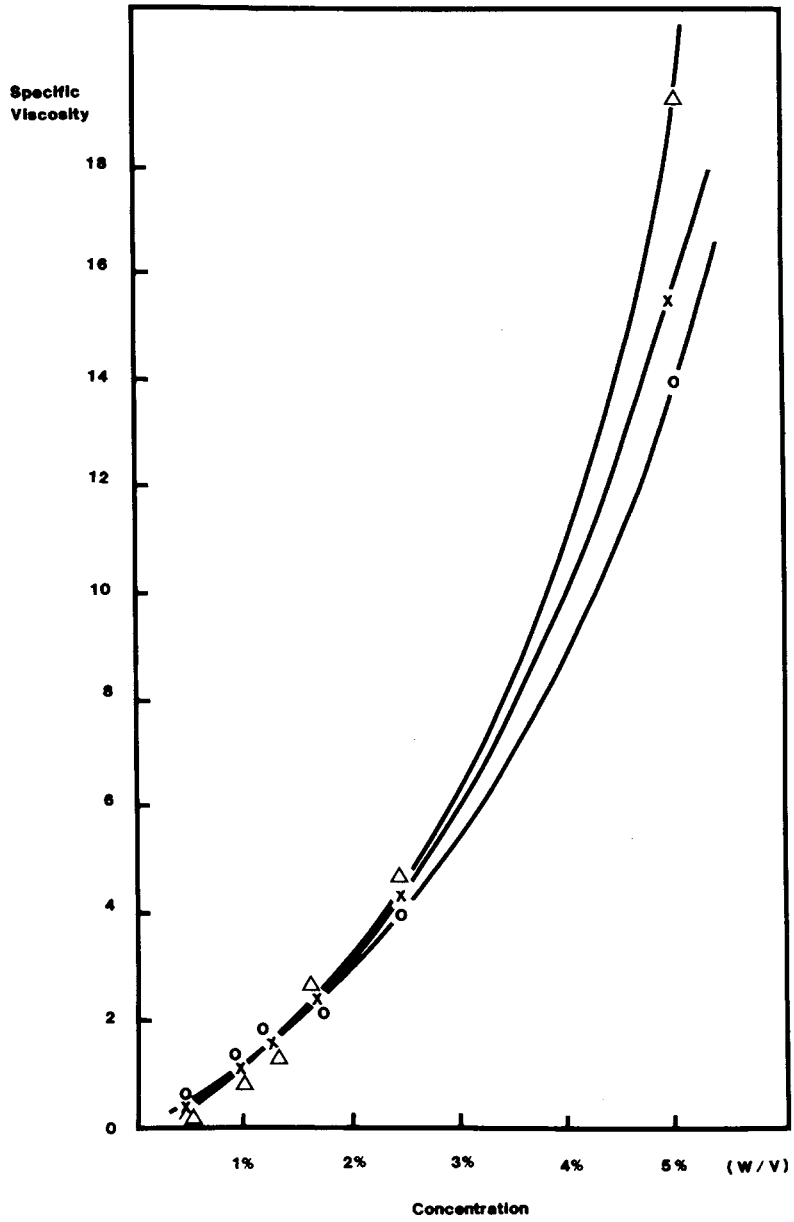

Fig. 5. Change of specific viscosity vs. PVC concentration for PVC in pure THF (○), 80/20 THF/toluene (X), and 60/40 THF/toluene (△).

energy Q can be calculated by using an Arrhenius-type law,[26] $\eta_{sp} = A \exp(Q/RT)$, where A is the preexponential factor, R the gas constant, and T the absolute temperature. The activation energy calculations were handled by linear regression analysis using a Xerox Sigma 9 Computer, and the results are shown in Table III.

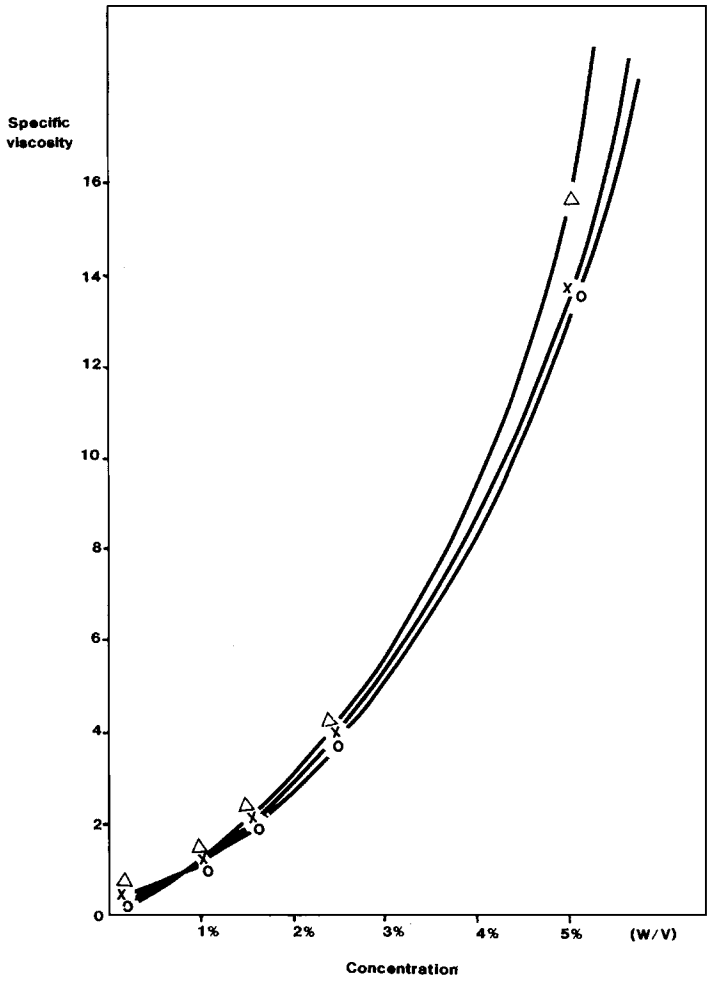

Fig. 6. Change of specific viscosity vs. PVC concentration for PVC in pure CHO (○), 80/20 CHO/toluene (X), and 60/40 CHO/toluene (△).

As shown in Table III, the activation energy of the PVC solutions increase with increasing toluene content in both the THF and CHO series. Thermodynamically, the activation energy is regarded as the height of the energy barrier required to displace a molecule from one equilibrium position to

TABLE III
Activation Energy (cal/mol) Q for Polymer-Chain Motion in Various Solvents at Nondilute Concentrations

Concn (W/V%)	THF	THF 80	THF 60	CHO	CHO 70	CHO 60
5.0	1090	1510	2100	1330	1900	2300
2.5	910	1060	1160	940	1650	1780
1.0	650	740	930	620	650	700

Note: In general, the experimental errors are less than 5%.

the next one during flow.[27] In other words, the polymer structure itself is associated with a higher energy barrier for polymer chain movements at higher toluene percentages in the above solvent mixtures. Theoretically, this means the interactions or the entanglement strength are enhanced by the thermodynamically less efficient solvent. This finding coincides with the previous one; therefore, it is reasonable to conclude that the movement of polymer chains is more restricted in poor solvents.

Determination of Solvent Evaporation

The solution properties affected by solvent differences have been discussed in the previous sections. Before discussing their influence on film properties, it is desirable to examine the solvent-evaporation process in order to understand the solvent composition during film formation. The evaporation of solvents from the PVC solutions was simulated as described in the experimental section. Although this approach could introduce some error, it should yield reasonable results because the evaporation of solvents mainly depends on the solvent nature and their surrounding conditions.[28]

Mathematically, the three calibration curves shown in Figure 2 are equivalent to the following expressions, respectively:

$$\text{for THF} \quad Y_{\text{THF}} = 0.7706X_{\text{THF}}$$
$$\text{for CHO} \quad Y_{\text{CHO}} = 0.8767X_{\text{CHO}}$$
$$\text{for toluene} \quad Y_{\text{toluene}} = 1.435X_{\text{toluene}}$$

where Y is the area ratio of the solvent to the standard and X is the weight ratio of the solvent to the standard. By using these calibration equations, the weight of the residue solvents can be easily calculated from the chromatogram; the volume of the solvents can also be approximated. The results are shown in Figures 7–14.

As can be seen from Figures 7–11, the evaporation rate of THF is much faster than that of toluene, so that only a small percentage of THF remains in the mixed solvents in the late stages of film formation. This feature is clearly shown in Table IV. It is obvious that the faster evaporation of THF during the film-formation period results in the mixed solvents becoming thermodynamically less efficient solvents, and, consequently, according to our previous discussions, leads to a greater reduction in polymer-chain motion in the concentrated solutions than would occur if the THF/toluene ratio remained constant during evaporation. In addition, the restricted motion of the polymer chains could result in poorer packing of the polymer chains which results in more porous films. Details are discussed in the following section.

The evaporation of the CHO series gives a completely different look during film formation than the THF series. As shown in Figures 12 and 13, the slope of the curves in Figure 12 is smaller than that of Figure 13; this means that the rate of toluene evaporated out of the mixed solvents is greater than that of CHO. Therefore, the volume percentage of CHO in the mixed solvents increases with time during the period of film formation. This feature is illustrated in Figure 14 and listed in Table V. As shown in Table V, the difference in the solvent composition is quite small during the

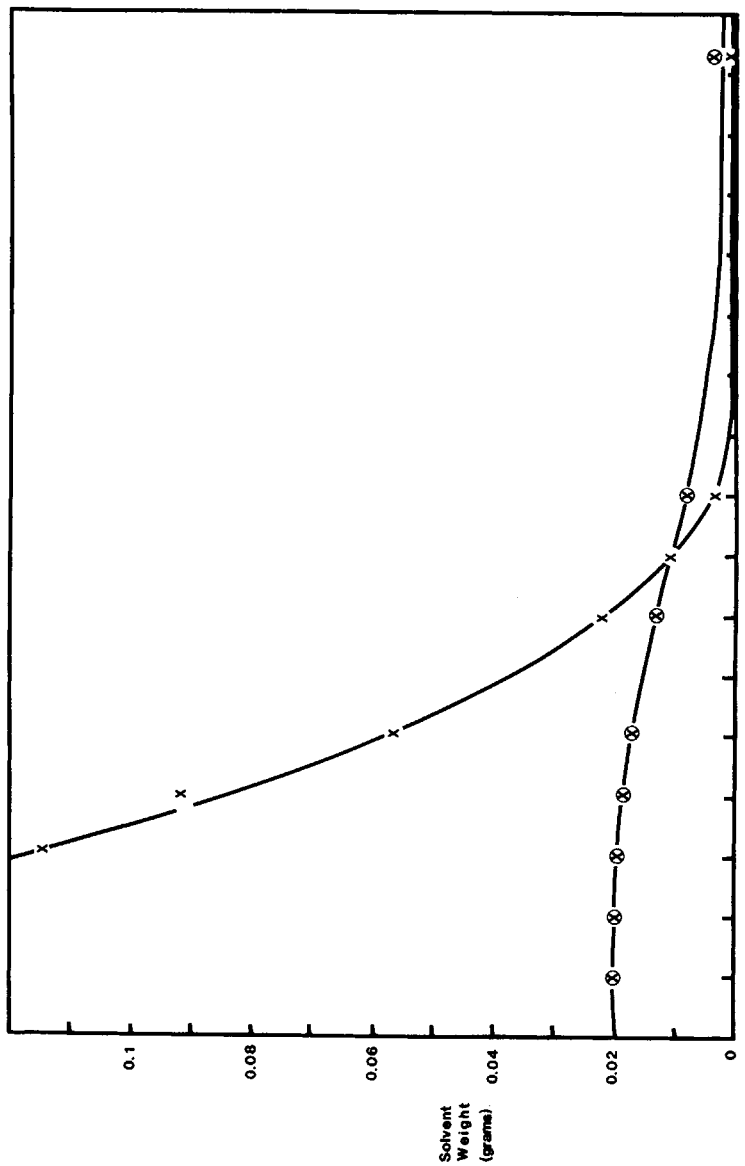

Fig. 7. Weight change of THF (X) and toluene (⊗) in THF 90 during film formation (initial sample weight of 0.221 g of 1% PVC in THF 90).

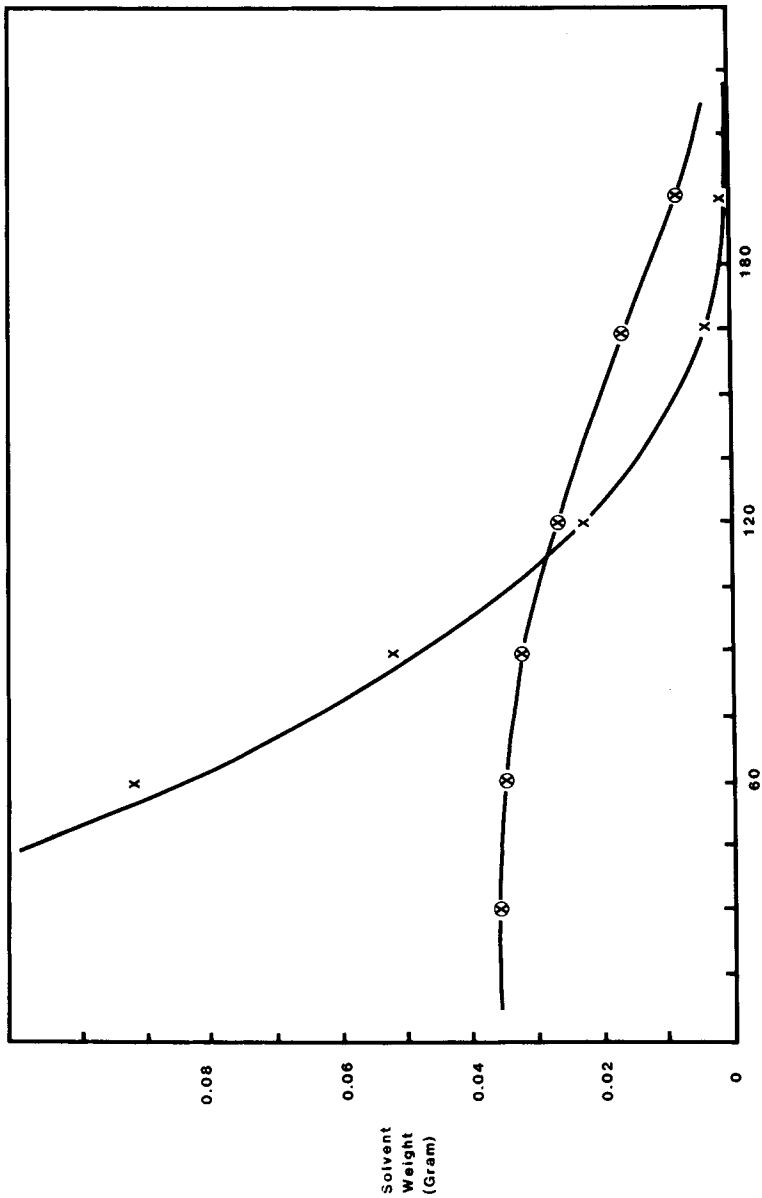

Fig. 8. Weight change of THF (X) and toluene (⊗) in THF 80 during film formation (initial sample weight of 0.221 g of 1% PVC in THF 80).

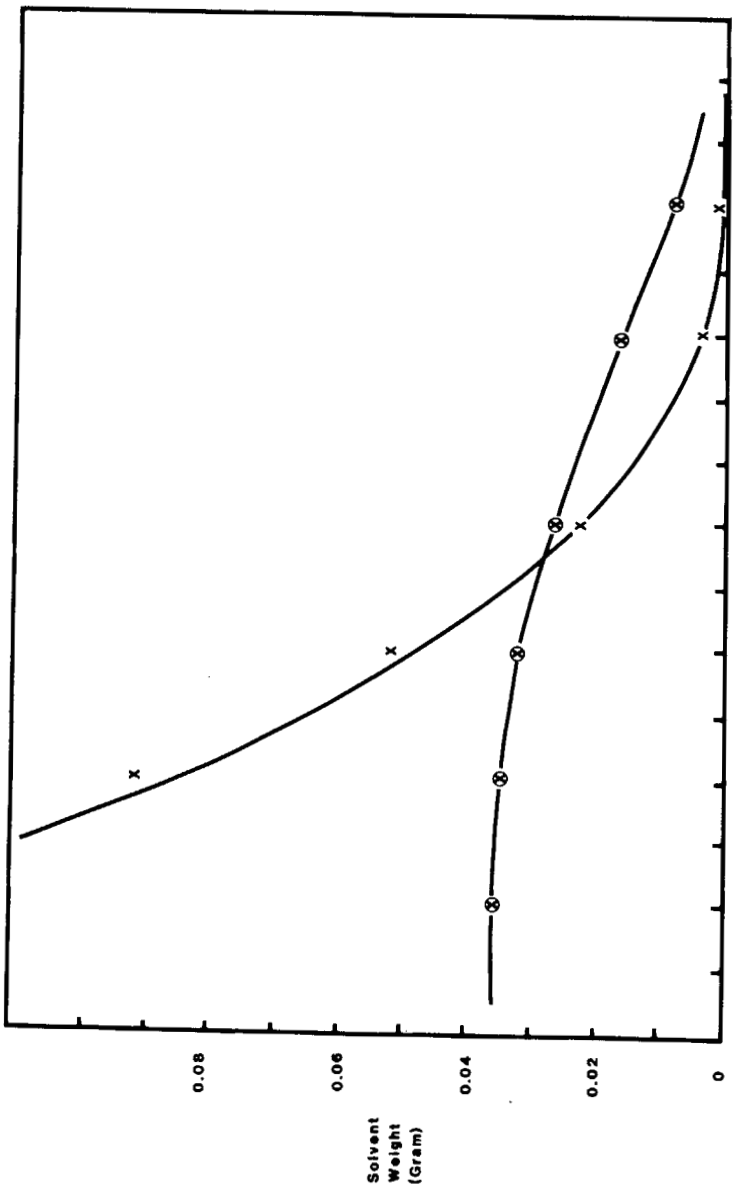

Fig. 9. Weight change of THF (X) and toluene (⊗) in THF 70 during film formation (initial sample weight of 0.221 g of 1% PVC in THF 70).

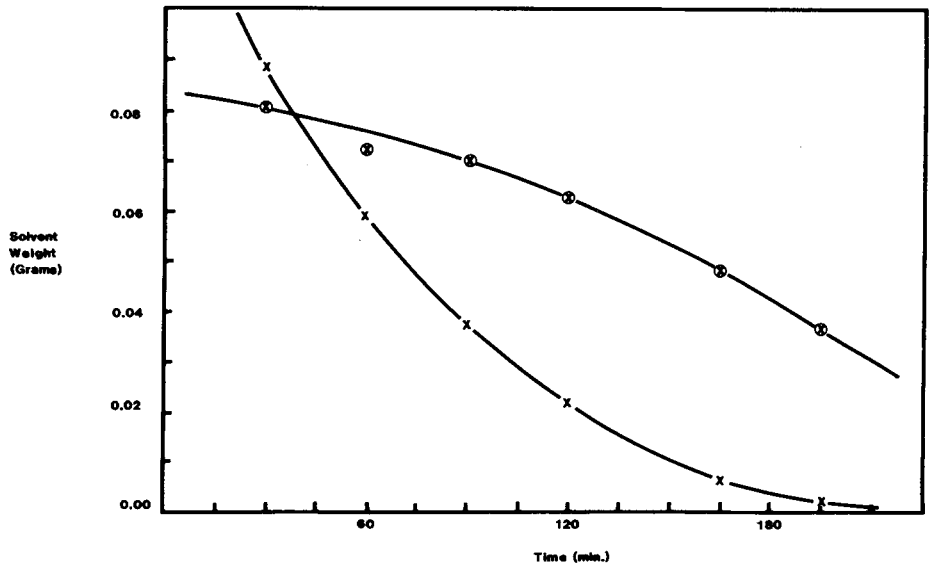

Fig. 10. Weight change of THF (X) and toluene (⊗) in THF 60 during film formation (initial sample weight of 0.221 g of 1% PVC in THF 60).

late stages of film formation. This factor makes the films formed from the CHO series have very similar surface properties. More details are discussed in the next section.

Surface Properties Characterized by IGC

The estimated thickness of the PVC coating on the inert support was ca. 420 Å. After the PVC-coated supports were dried and conditioned, the presence of residual solvent was not detectable by the GC method described previously. Thus, residual solvent is not expected to influence the IGC data.

It is well known that polymer–probe interaction, polymer crystallinity, and the porousity of the structure are the most important factors which determine the magnitude of the retention volume in IGC. In this investigation it is assumed that (1) the polymer–probe interaction is the same for all measurements because the same polymer (PVC) and probe (dodecane) were employed for each measurement and (2) the effect of solvents on the crystallinity or comformational states of cast PVC was not significant because the ratio of intensity of 1427 cm^{-1}/1435 cm^{-1} obtained from ATR-IR measurements is nearly the same for PVC films cast from the THF and CHO series. Therefore, the porousity of the PVC is considered to be the most important factor affecting the retention volume.

Based on a mean-square end-to-end distance calculation of a freely rotating chain the probe, dodecane, has an average radius gyration of 2.92 Å. Theoretically, any porous site or microvoid which has a diameter larger than 6 Å should be accessible to the probe. The probe can penetrate into the bulk texture of the coated films. Hence, the information gathered from

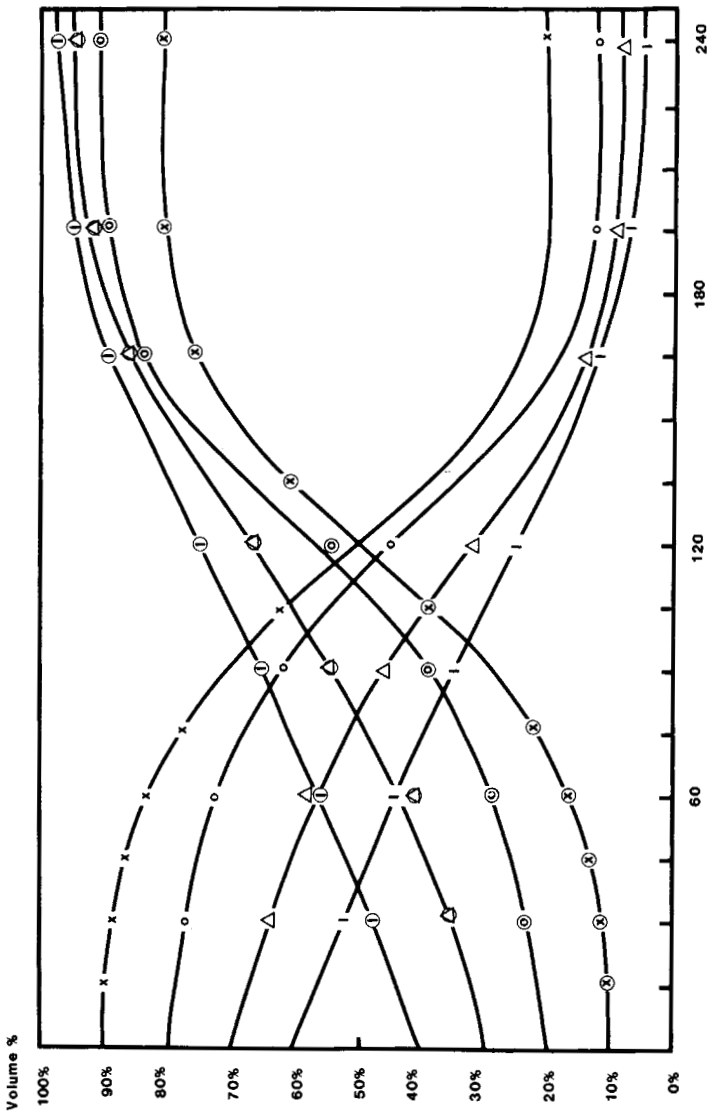

Fig. 11. Change of vol % of THF and toluene in various solutions during the film formation period: (X) THF in THF 90 soln; (⊗) toluene in THF 90; (○) THF in THF 80 soln; (◉) toluene in THF 80; (△) THF in THF 70; (▲) toluene in THF 70; (|) THF in THF 60; (▮) toluene in THF 60.

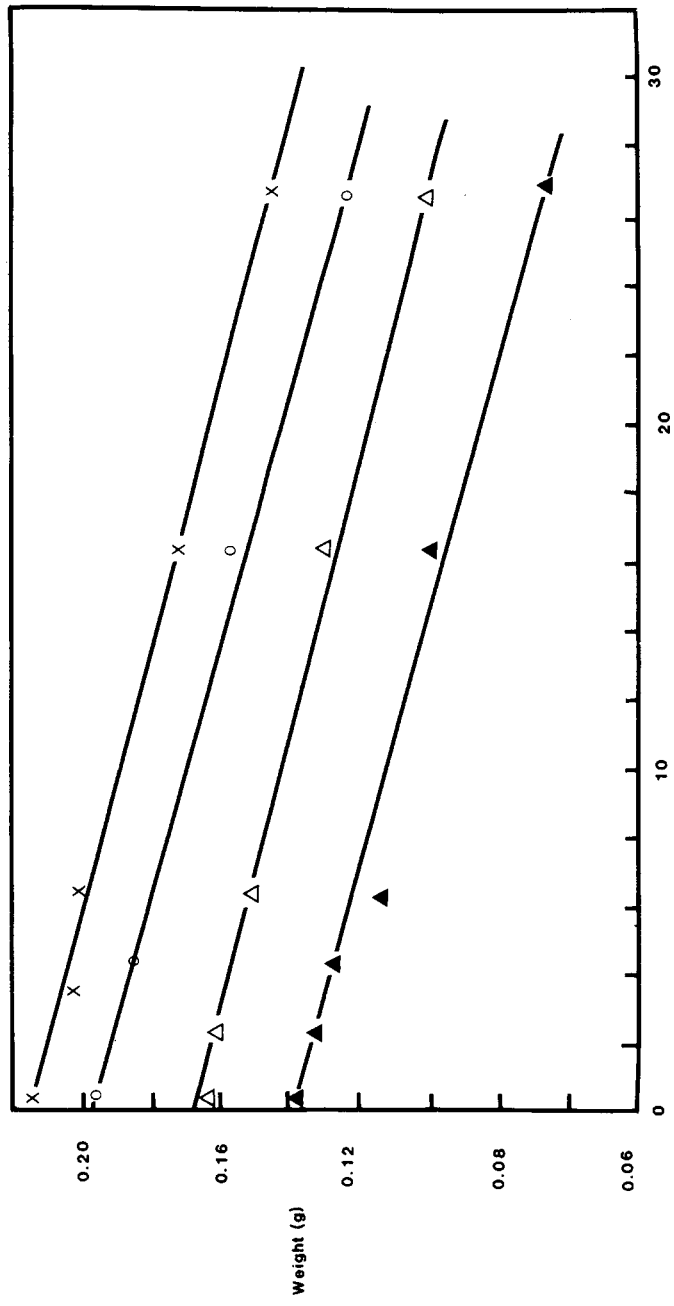

Fig. 12. Change of weight of cyclohexanone in various solutions during the period of film formation (initial sample weight of 0.231 g of 1% PVC solution): (X) CHO in CHO 90 solution; (○) CHO in CHO 80 solution; (△) CHO in CHO 70 solution; (▲) CHO in CHO 60 solution.

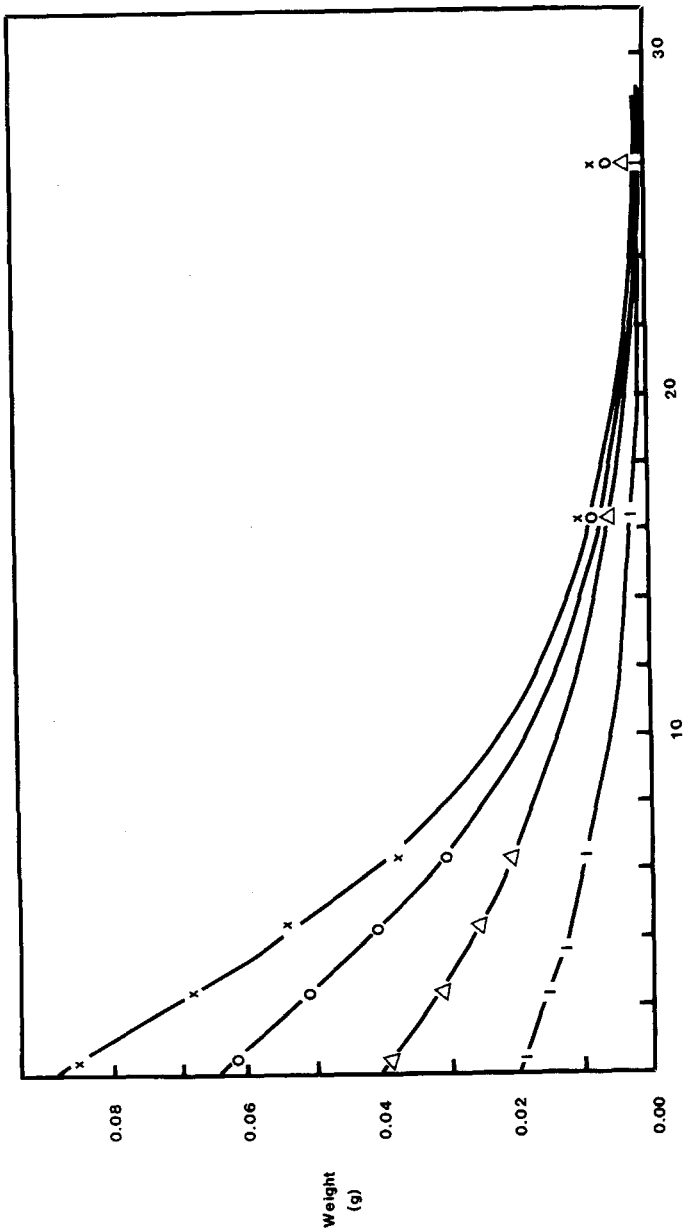

Fig. 13. Change of weight of toluene in various solutions during the period of film formation: (X) toluene in CHO 90 solution; (○) toluene in CHO 80 solution; (△) toluene in CHO 70 solution; (|) toluene in CHO 60 solution.

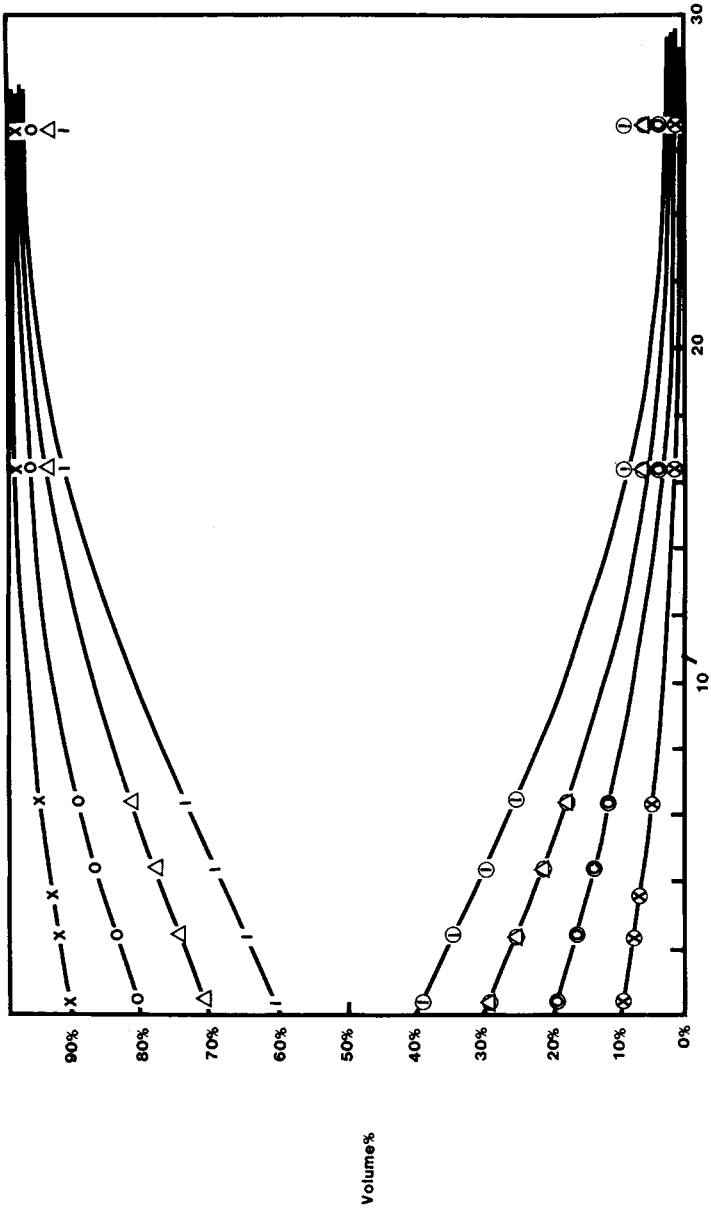

Fig. 14. Change of vol % of CHO and toluene in various solutions during the period of film formation: (X) CHO in CHO 90 solution; (⊗) toluene in CHO 90; (○) CHO in CHO 80 solution; (●) toluene in CHO 80; (△) CHO in CHO 70 solution; (▲) toluene in CHO 70; (|) CHO in CHO 60 solution; (①) toluene in CHO 60.

TABLE IV
Change of Vol % of THF in the Remaining Solvent for the THF-Series Solvents with Elapsed Time during Film Formation

Solvent	Initial	1 h	2 h (vol %)	3 h	4 h
THF	100	100	100	100	100
THF 90	90	84	50	21	20
THF 80	80	73	46	13	12
THF 70	70	57	33	11	8
THF 60	60	44	26	8	5

IGC should represent an average property of the polymer texture. It should be noted that the equation for calculating the retention volume is based on the weight average, not the surface area average. Thus, a sample with a larger average porousity will result in the larger retention volume.

The inverse phase gas chromatographic data and results are listed in Table VI. Here the random errors were calculated based on a 95% confidence limit in three measurements.[29] In general, the random errors are closed to 4%. As shown in Table VI, the specific retention volumes V_g^0 for the polymer coated supports from the CHO-series solvents do not exhibit a large variation, while the THF series show a significant difference for each solution.

Table VII lists the volume percent change in toluene during film formation along with the specific retention volumes of the resultant film surface. From Table VII, one will notice that there is a direct correlation between solvent composition and surface property. Generally speaking, the larger retention volumes result from the higher toluene content. In the THF series, the value of V_g^0 for a film from THF 90 (90% THF/10% toluene) is significantly larger than a film from pure THF. The V_g^0 increases as the toluene content increases the THF series. This change in V_g^0 cannot be persuasively interpreted by just using the composition difference in initial solvents, but it can be clearly understood from the change of solvent composition during the film formation period. As shown in Table VII, a considerable difference in the solvent compositions between pure THF and THF 90 exists in the later stages of film formation, and the toluene even

TABLE V
Change of Vol % of CHO in the Remaining Solvent for the CHO-Series Solvents with Elapsed Time during Film Formation

Solvent	Initial	4 h	8 h (vol %)	12 h	16 h	20 h
CHO	100	100	100	100	100	100
CHO 90	90	94	96	97	98	99
CHO 80	80	87	91	94	96	97
CHO 70	70	78	84	90	93	96
CHO 60	60	69	77	85	91	95

TABLE VI
Data Collected from IGC Experiment for the Calculation of Specific Retention Volumes (V_g^0)

Solvent	Polymer loading (g)	Inlet pressure (cm Hg)	Retention time (min)	V_g^0 (mL g^{-1})
THF	0.0443	116.1	23.9	5460 ± 200
THF 90	0.0385	116.0	24.9	6550 ± 240
THF 80	0.0433	113.7	28.1	6640 ± 190
THF 70	0.0397	110.6	27.1	7120 ± 300
THF 60	0.0384	111.3	27.3	7400 ± 260
CHO	0.0358	112.3	19.7	5690 ± 250
CHO 90	0.0367	113.7	20.7	5700 ± 220
CHO 80	0.0320	115.3	19.8	6270 ± 300
CHO 70	0.0353	114.2	20.7	6000 ± 290
CHO 60	0.0347	112.7	21.3	6340 ± 260

dominates the solvent mixture in quantity. This change will make the THF 90 become a much poorer solvent as evaporation progresses as compared with its initial solvent power. Consequently, the polymer-chain movement during the film-formation period will be more restricted than that in pure THF, and make the uniform packing of polymer chains more difficult. This results in the formation of more porous films.

During the later stages of film formation, the relaxation times of the polymer chains are probably not rapid enough for the chains to achieve equilibrium conformations. The glass transition temperature for PVC is 83°C which is well above room temperature; thus, during the final stages of solvent loss the polymer–solvent mixture is below T_g. The retention properties of the polymer in a nonequilibrium conformation is probably different than the retention for equilibrium conformations. It is difficult to

TABLE VII
Comparisons of the Vol % Change of Toluene during Film Formation with the Specific Retention Volumes (V_g^0) of the Film Surface

Solvent	Vol % of toluene				V_g^0 (mL g^{-1})
	Initial	2 h	3 h	4 h	
THF	0	0	0	0	5460
THF 90	10	50	79	80	6550
THF 80	20	54	87	88	6640
THF 70	30	67	89	92	7120
THF 60	40	74	95	95	7400
	Initial	8 h	12 h	16 h	
CHO	0	0	0	0	5690
CHO 90	10	4	3	2	5700
CHO 80	20	9	6	4	6270
CHO 70	30	16	10	7	6000
CHO 60	40	23	15	9	6340

separate the effects on V_g^0 of nonequilibrium chain conformations and film porousity since they are somewhat interrelated during the later stages of film formation. The results of annealing the samples are presented below. X-ray radial distribution analysis is being evaluated as a means of determining the average chain conformation of films prepared from the different solvent mixture.

In the case of the CHO series, the solvent compositions are different initially, but these differences are reduced considerably during the film formation period. This change reduces the differences in solution properties and causes the packing ability of the polymer chains to become similar. Although differences in V_g^0 still exist, they are much less than for the THF-series films.

When comparing the value of V_g^0 of polymer surfaces in Table VII, it is noticed that the difference between pure THF and pure CHO is within experimental errors. This finding shows that both solvents provide good packing ability of the polymer chains. As shown in Table III, the activation energy for polymer-chain motion is only slightly higher in CHO than in THF, whereas, as the percent toluene increases, the activation energy increases significantly which reduces the polymer packing efficiency in a film.

Annealing Effects on the Surface Properties

After the columns have been annealed at 90°C for 3 h, which is above the glass transition temperature of 83°C, the specific retention volumes change significantly as shown in Table VIII. The specific retention volumes of THF series exhibit larger changes than those of CHO series. This is probably because a larger number of microvoids are removed from the THF-series films during annealing.[30]

CONCLUSIONS

In this investigation, the solvent effects on the surface properties of poly(vinyl chloride) films were studied by using inverse phase gas chromatograph; the solution properties of PVC at higher concentrations were

TABLE VIII
Comparisons of Specific Retention Volumes Before and After Aging at 90°C for 3 h

Solvent	Before aging	After aging	Difference
THF	5460	5250	210
THF 90	6550	6020	530
THF 80	6640	6130	520
THF 70	7120	6680	440
THF 60	7400	6910	490
CHO	5690	5600	90
CHO 90	5700	5600	100
CHO 80	6270	6090	180
CHO 70	6000	5780	220
CHO 60	6340	6130	210

measured; the evaporation of solvent mixtures were also simulated. Instead of using the intrinsic viscosity to relate polymer-chain dimension, the concept of the mobility of polymer chains is introduced to interpret the results. The conclusions which can be drawn from this study are:

1. At higher concentrations, polymer chain–polymer chain interactions become stronger when thermodynamically less efficient solvents are used. The stronger interactions limit the motion of polymer chains and hence reduce the packing ability of polymer chains during film formation. This characteristic leads to a more porous structure of the polymer films.

2. The solvent balance is important to the film formation. Especially, the solvent composition at the later period of film formation has a critical influence on the surface properties of the film. In the THF-series solutions a larger percent of toluene remained in the later stage of film formation resulting in a more porous surface structure. However, the faster evaporation of toluene in the CHO series keeps the surface structure less porous.

3. Annealing of polymer films above T_g can reduce the porous structure and improve the surface properties.

4. The concept of activation energy for polymer-chain motion was introduced to interpret the packing ability of polymer chains in terms of the strength of polymer chain–polymer chain interactions.

References

1. D. T. Clark and W. J. Feast, *Polymer Surface*, Wiley-Interscience, Chichester, New York, 1978, p. 309.

2. Reference 1, p. 287.

3. Lieng-Huang Lee, *Characterization of Metal and Polymer Surface*, Academic, New York, 1977, Vol. 2, p. 147.

4. Reference 3, p. 249.

5. K. R. Buser, *J. Coatings Tech.*, **54**, 689 (1982).

6. O. Smidsrod and J. E. Guillet, *Macromolecules*, **2**, 272 (1969).

7. H. P. Schreiber and M. D. Croucher, *J. Appl. Polym. Sci.*, **25**, 1961 (1980).

8. J. P. Cotton, D. Decker, H. Benoit, B. Farnoux, J. Higgins, G. Jannink, R. Ober, C. Picot, and J. des Choizeaux, *Macromolecules*, **7**, 863 (1974).

9. M. Daoud, J. P. Cotton, B. Farnoux, G. Jannink, G. Sanna, H. Benoit, R. Duplessix, C. Picot, and P. G. Genes, *Macromolecules*, **8**, 804 (1975).

10. H. Hayashi, F. Hamada, and A. Nakajima, *Macromol. Chem.*, **178**, 827 (1977).

11. H. Hayashi, F. Hamada, and A. Nakajima, *Polymer*, **18**, 638 (1977).

12. Toyohiko Yoshida, *Prog. Org. Coatings*, **1**, 73 (1972).

13. M. R. Cannon, *Anal. Chem.*, **32**, 355 (1960).

14. W. R. Krigbaum and P. J. Flory, *J. Polym. Sci.*, **11**, 37 (1953).

15. H. M. McNair, and E. J. Bonelli, *Basic Gas Chromatography*. Varian Instruments, Sunnyvale, California, 1969, p. 154.

16. W. R. Supina, *The Packed Column in Gas Chromatography*, Supelco, Bellefonte, Pennsylvania, 1979, p. 95.

17. Koich Ito, Noiriyuki Usami, and Yuya Yamashita, *Macromolecules*, **13**, 216 (1980).

18. J. M. Braum, M. Cutajar, J. E. Guillet, H. P. Schreiber, and D. Patterson, *Macromolecules*, **10**, 864 (1977).

19. K. S. Gandhi, and M. C. Williams, *J. Polym. Sci., Part C*, **35**, 2111 (1971).

20. Yoshinobu Isono, and Mitsuru Nagasawa, *Macromolecules*, **13**, 862 (1980).

21. R. T. Bailey, A. M. North, and R. A. Pethrick, *Molecular Motion High Polymers*. Clarendon, Oxford, 1981, Vol. 18.

22. Reference 21, Chap. 7.

23. C. A. Herb and J. R. Overton, *Proceedings of the Ninth Water-Borne and Higher-Solids Coatings Symposium*, G. C. Wildman and R. E. Burks, Eds., Univ. of Southern Mississippi Press, Hattiesburg, MS, 1982, Vol. 45.

24. H. Kajiura, Y. Ushiyama, T. Fujimoto, and M. Nagasawa, *Macromolecules*, **11**, 894 (1978).

25. Y. Isono, T. Fujimoto, H. Kajiura, and M. Nagasawa, *Polym. J.*, **12**, 363 (1980).

26. P. W. Atkins *Physical Chemistry*, Freeman, San Francisco, 1978, p. 776.

27. W. J. Moore, *Physical Chemistry*, Prentice-Hall, Englewood Cliffs, NJ, 1972, Chap. 19.

28. R. W. Tess, Ed., *Solvent Theory and Practice*, American Chemical Society, Washington, DC, 1973, Chap. 2.

29. E. Kreyszig, *Advanced Engineering Mathematics*, Wiley, New York, 1972, p. 754.

30. L. E. Alexander, *X-Ray Diffraction Methods in Polymer Science*, Wiley, New York, 1969, p. 331.

Received August 8, 1984
Accepted February 7, 1985